

Mechanical properties of polycarbonate-TiO₂ nanocomposite film

Nima Shahbazi¹, Babak Jaleh^{1*} & Amir Momeni²

¹Physics Department, Bu-Ali Sina University, Hamedan, Iran

²Materials Science and Engineering Department, Hamedan University of Technology, Hamedan, Iran

Received 6 April 2014; revised 4 August 2015; accepted 5 November 2015

The mechanical properties of polycarbonate-TiO₂ nanocomposite films have been investigated by conducting tensile tests and hardness measurements. The elastic modulus of the composite increased with increasing the weight fraction of particle, especially over 0.8 wt%. The X-ray diffraction results (XRD) show that the increase of strength is accompanied by decrease in intensity of amorphous polycarbonate and appearance of the peak of anatase. The theoretical models proposed by Guths-Smallwood, Einstein, Kerner and Cohen-Ishai are used but only the first model provided better results and is modified for the studied composite. The law of mixture is used to calculate the contribution coefficients of the constituents and the results of this modeling provided the acceptable precision. Peak stress and strain has been increased with increasing TiO₂ nanoparticles content while the stress and strain corresponding to the fracture point did in opposite. It is attributed to the influence of particles on the plastic weakening of the composite.

Keywords: Nanocomposite, Tensile testing, Modeling, TiO₂ nanoparticles, Polycarbonate-TiO₂ nanocomposite film

1 Introduction

Polymer nanocomposites have been studied due to their superior properties, such as enhanced stiffness, hardness and strength. The properties of polymer nanocomposites are mostly a simple combination of the properties of incorporated inorganic nanoparticles and polymeric matrix. However, sometimes completely new characteristics may appear due to synergistic effects¹⁻⁴.

Polycarbonate⁵ (PC) is used in many fields of industrial applications because of its excellent physical and mechanical properties, such as high toughness and transparency. It is a promising polymer having high transparency in the visible spectral range, which is used in many fields of life, such as airplane windows. New polycarbonate nanocomposites have been developed with the idea of improved physical, thermal, mechanical, electrical or optical properties of the base polymer⁶⁻⁸. Based on this idea, the dispersion of various nanomaterials in the polymer matrices is growing fast and opening new horizons to the polymeric materials.

Titanium dioxide (TiO₂) is one of those very important filler materials that are used in polymer nanocomposite materials. It is widely used in several applications, including optoelectronic and photocatalytic

activities, electrochromic applications, hydrogen storage and gas sensors⁹⁻¹².

Hsieh *et al.*¹³ reported the effect of clay on the mechanical behaviour and melt state linear viscoelastic properties of intercalated PC nanocomposite. The effect of aluminium oxide (Al₂O₃) powders on improving the mechanical and thermal properties of polyethylene has been investigated by Tavman¹⁴. Similarly, the tensile properties of Kaolin-polypropylene¹⁵ and CaCO₃-polypropylene nanocomposites¹⁶ have been investigated. The effect of particle shape on the mechanical properties of filled polymers¹⁷ has also been studied. Among the investigated polymer nanocomposites, the combination of TiO₂ and PC is of industrial importance due to the interesting individual physical and mechanical properties of the constituents. Although the physical properties of PC-TiO₂ nanocomposite have been analyzed in the past works, its mechanical properties, especially at low mass fractions of TiO₂ nanoparticles, have been less documented in the literature. Hence, the present investigation is devoted to deal with the mechanical properties of PC-TiO₂ nanocomposite and to provide a way of modeling the mechanical behaviour of this material.

2 Experimental Procedure

Polycarbonate samples (PC) (General Electric (GE) Company, USA) and titanium dioxide (TiO₂)

*Corresponding author
(E-mail: bkjaleh@yahoo.com, jaleh@basu.ac.ir)

(Degussa Company, Germany) powders of 30 nm with 80% anatase and 20% rutile phases are used. Initially, PC was dissolved in dichloromethane. Then, TiO₂ nanoparticles were added to the solution with different weight percentages of 0.4, 0.8, 1, 1.5 and 2% and the mixture was sonicated with an ultrasonic probe (SONOPULS) for 10 min to facilitate thorough mixing. Nanocomposite and PC films were obtained by solvent evaporation method at 40°C in oven. The film thickness (200 μm) was kept constant.

The structure of samples was studied using X-ray diffraction on a Philips Powder Diffractometer type PW 1373 goniometer. The XRD apparatus was equipped with a graphite monochromator crystal. The X-ray wavelength was 1.5405 Å and the diffraction patterns were recorded over the 2θ range of 10°- 60° with a scanning speed of 2° per min. Vickers micro hardness tests were carried out using a BUEHLER (model 60044 USA) micro hardness tester with an attached microscope. The samples were indented with a Vickers diamond pyramid indenter having a square base and 136° pyramid angle. The average hardness values of four heats for each sample were taken. The hardness was measured by applying 50 g load for a constant loading time of 30 s. The samples for tensile testing were prepared according to the ASTM E8M standard. Tensile testing was performed by a SANTAM machine at the ambient temperature and the results of force-extension were used to calculate the stress-strain curves. The tensile tests were performed under the constant strain rate of 0.001 s⁻¹.

3 Results and Discussion

The stress-strain curves of PC filled with different weight fractions of TiO₂ nanoparticles are shown in Fig. 1. All the flow curves represent steep increase of stress up to a peak that is associated with de-cohesion of primary bonds between the polymeric molecules and can be regarded as the yield point of the material. Prior to yield, molecules uncoil and undergo segmental elongations without relative movement, which is irreversible. After the peak, plastic deformation is accompanied by flow softening until the start of realignment of molecule chains¹⁸. It can be roughly observed that TiO₂ nanoparticles have had a more remarkable effect on the strength than the ductility of the studied polymer matrix composites (PMC).

Due to the applicability of such PMCs as self cleaning translucent parts¹⁹, their elastic properties are more noticeable than the plastic ones. This is why the

elastic properties of such materials have drawn more attention in the literature²⁰⁻²². As most of polymers are visco-elastic materials, their behaviour under time-dependent creep or stress relaxation is more crucial²³⁻²⁵ than tensile testing. However, static tensile testing is often used to determine the elastic modulus (E) as a function of other variables, such as the weight fraction of reinforcing particles. Figure 2 shows the variation of E with the weight fraction of TiO₂ nanoparticles. The PMCs are actually dilute ones with low additions of TiO₂ (actually below 2 wt%) that are especially interesting from economical point of view. The remarkable improvement of elastic modulus with increasing TiO₂ nanoparticles is simply attributed to the partly or completely immobilization of molecular chains of polycarbonate due to the interaction with nanoparticles. This actually means a dispersion hardening phenomenon that stems from the second phase particles, which limit the flowing of molecules and postpones the permanent or plastic deformation.

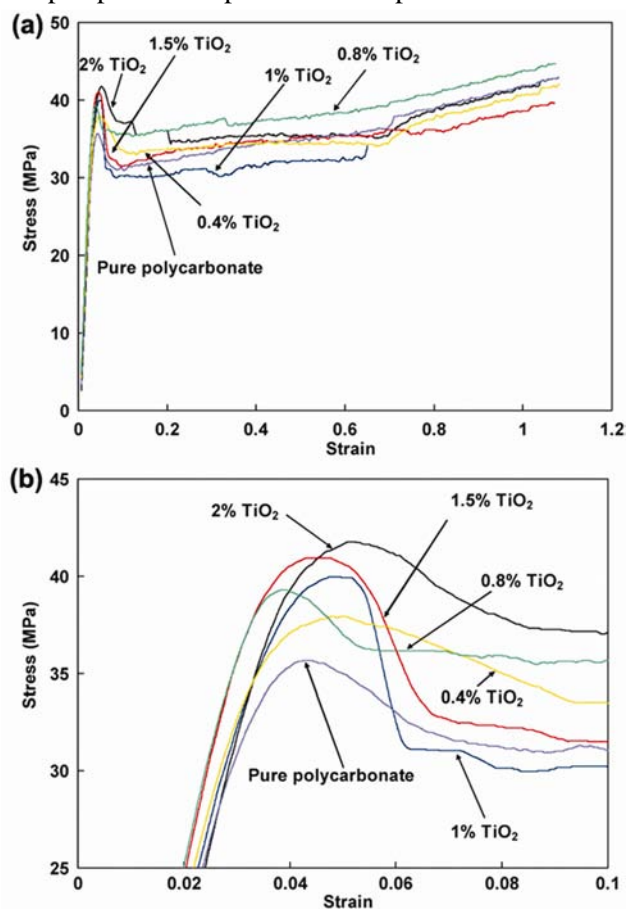


Fig. 1 – (a) Stress-strain curves of the polycarbonate filled with different weight fractions of TiO₂ nanoparticles, (b) magnified view of the peak region in (a)

Moreover, higher E may be interpreted as more brittle material that accommodates lower elastic strain at a constant applied stress. This is a real concern that should be verified by considering the variation of peak strain with the weight fraction of TiO₂ nanoparticles.

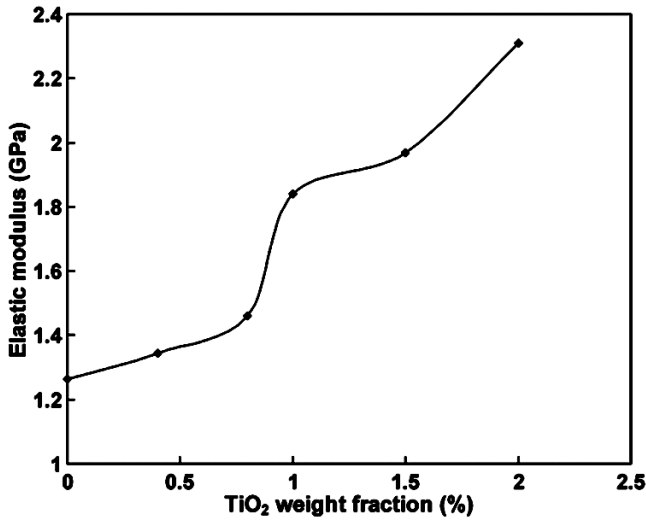


Fig. 2 – Plot of the variation of elastic modulus with the weight fraction of TiO₂ nanoparticles

The evolution of phases in PC with the increase of TiO₂ nanoparticles has been investigated by XRD analyses as shown in Fig. 3. It is evident that at low contents of TiO₂ nanoparticles (up to 0.8 wt%), the diffraction pattern is characterized by a single peak that corresponds to the amorphous structure of PC. However, with increase in the content of TiO₂ nanoparticles, actually over 1 wt%, other peaks appear at $2\theta = 25.2^\circ$ and 48.1° that correspond to (101) and (200) planes of anatase²⁶, respectively. As the weight fraction of nanoparticles rises, the intensity of TiO₂ peak increases and that of amorphous matrix decreases. These observations signify a change in the microstructure of polycarbonate from short range order towards long range order or partial crystallization. However, a change in the adhesion quality of particles to the matrix may be as important as the change in the structure of polymeric molecules around TiO₂ nanoparticles. The current results are in agreement with the literature that reported considerable increase of strength of PMCs with crystallization²⁷. Therefore, the remarkable increase of E value with increasing TiO₂ nanoparticles from 0.8 wt% to 1 wt% in Fig. 2 can be discussed with the corresponding changes in the microstructure of the

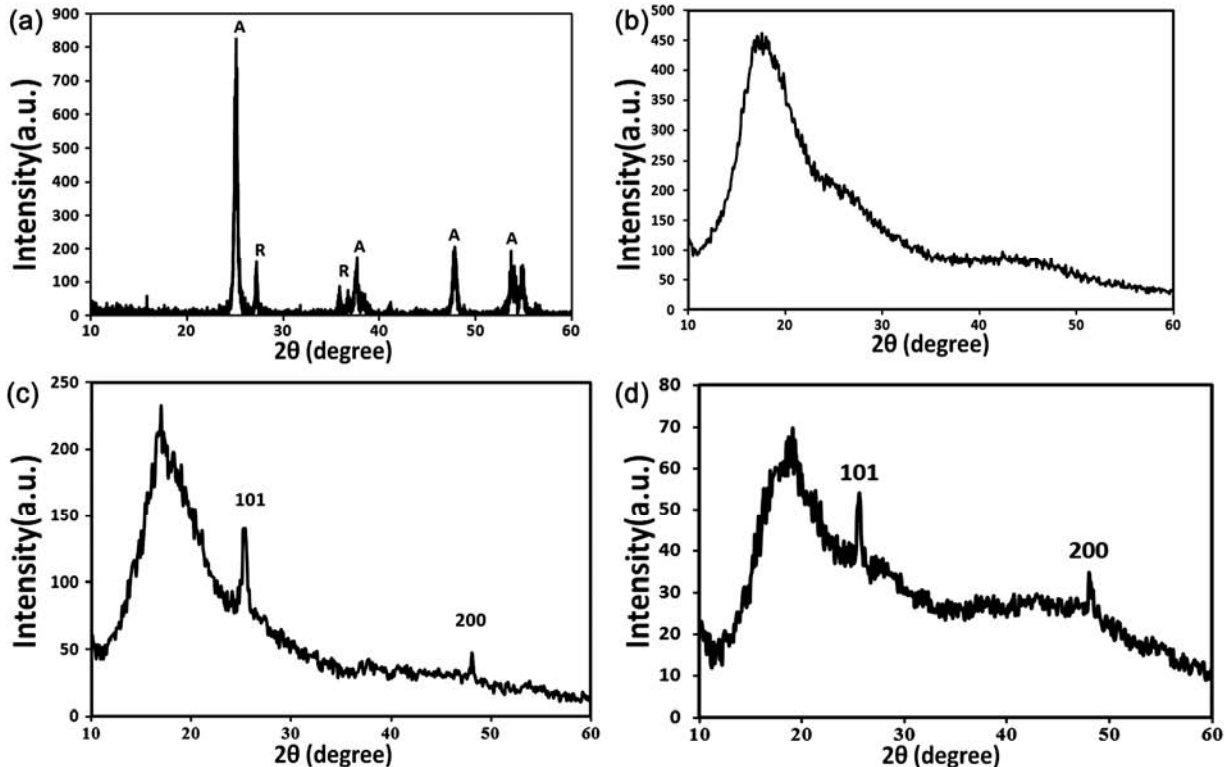


Fig. 3 – X-ray diffraction patterns of: (a) TiO₂ powder, (b) pure PC, (c) PC-TiO₂ nanocomposites (1 wt%), and (d) PC-TiO₂ nanocomposites (2 wt%)

material. The same observations have been made from the variation of micro hardness with the content of TiO₂ nanoparticles as shown in Fig. 4. Similar to the results of *E* in Fig. 2, micro hardness values show a sharp change around 0.8 wt% of TiO₂ nanoparticles. As hardness value reflects the resistance of material to plastic deformation, the remarkable increase of hardness shows the improvement of stiffness at higher content of TiO₂ nanoparticles.

3.1. Modeling of elastic module

During past decades, several models have been proposed to predict the mechanical properties of filled polymers based on the assumptions about the behaviour of microstructural constituents (matrix and reinforcing material) and the bonding quality^{16,28,29}. The experimental results of a given PMC can, therefore, be compared with the models to provide better understanding of the behaviour of microstructural constituents. Some of the models proposed to predict the elastic modulus of a PMC are as follows:

(i) Einstein's equation for case of perfect adhesion between the isolated particles and the matrix^{14,16}:

$$\frac{E_c}{E_p} = 1 + 2.5 \dots (1)$$

where, *E_c* and *E_p*, are the elastic modulus of composite and PC, respectively; and *v_p*, the weight fraction of nanoparticles.

(ii) Modified Kerner's equation for the case of adhesion between the constituents¹⁶:

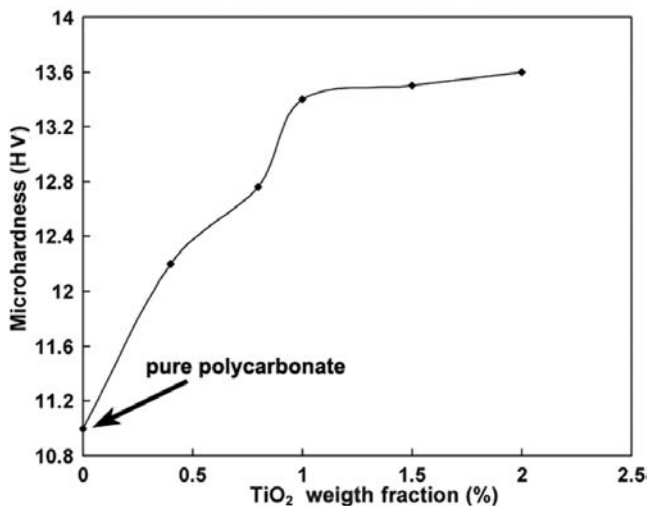


Fig. 4 – Variation of micro hardness of the composite with the content of TiO₂

$$\frac{E_c}{E_p} = 1 + \frac{15(1 - \nu_p)}{8 - 10\nu_p} \cdot \frac{\dots}{1 - \dots} \dots (2)$$

where, *v_p*, is the Poisson's ratio of PC.

(iii) Einstein's equation for poor adhesion¹⁴:

$$\frac{E_c}{E_p} = 1 + \dots (3)$$

(iv) Guth and Smallwood's equation, again for poor adhesion between matrix and nanoparticles¹⁵:

$$\frac{E_c}{E_p} = 1 + 2.5 \dots + 14.1 \dots^2 \dots (4)$$

(v) Cohen and Ishai's equation for bulk cubic fillers, using the modulus ratio of filler to matrix¹⁵ (*m*=*E_f*/*E_p*):

$$\frac{E_c}{E_p} = 1 + \frac{\dots}{\left(\frac{m}{m-1}\right)^{-1/3}} \dots (5)$$

Figure 5 (a-e) shows the comparison of the experimental and modeling data predicted from the above models. In the models, *E_p* was adopted as 1.26 GPa determined from the tensile data of pure polycarbonate as shown in Figs 1 and 2. The ability of different methods proposed in Eqs (1)-(5) to model the flow curves was evaluated and the mean square error (MSE) was calculated by Eq. (6) and reported on the corresponding curves:

$$MSE = \frac{1}{N} \sum_{i=1}^N (t_i - y_i)^2 \dots (6)$$

where, *t_i*, is the experimental value; and *y_i*, the model output. It is observed that over the whole range of TiO₂, the models considering the poor adhesion of nanoparticles to the matrix provide lower error values. In addition, the experimental values and the modeling outputs are more relevant at low contents of TiO₂ (actually below 0.8 wt%) that is likely due to more adhesion between the nanoparticles and the matrix. Among the mentioned models, Guths and Smallwood's equation¹⁵ [Eq. (4)] exhibits the lowest MSE value and therefore, provides better correlation with the experimental data. This formulation can be modified to better fit the behaviour of studied PMC. As shown in Fig. 6, the Eq. (7) with modified coefficients gives a reasonable approximation of the experimental data:

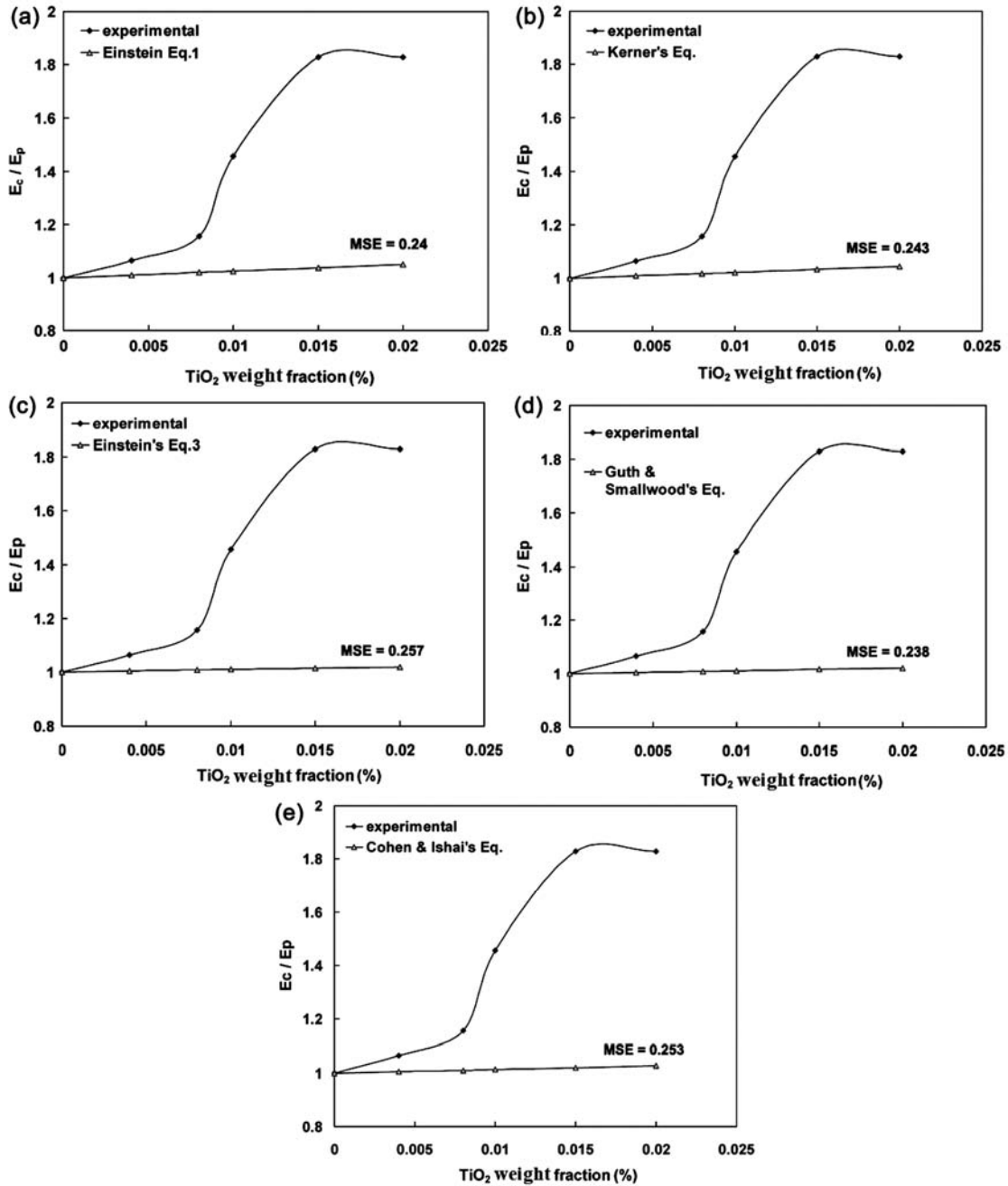


Fig. 5 – Plot of relative tensile modulus (E_c/E_p) against weight fraction of TiO₂ [Experimental data points are compared with the predicted ones by: (a) Einstein's equation for perfect adhesion [Eq. (1)]; (b) Kerner's equation for adhesion [Eq. (2)]; (c) Einstein's equation for poor adhesion [Eq. (3)]; (d) Guth and Smallwood's equation for poor adhesion [Eq. (4)]; and (e) Cohen and Ishai's equation for bulk cubic fillers [Eq. (5)]

$$\frac{E_c}{E_p} = 1 + 33.6 \cdot \left(\frac{w}{100}\right)^2 \dots (7)$$

Based on the law of mixture, the mechanical and/or physical properties of a composite material can be described as the weighted average of the mechanical

and/or physical properties of its constituents. This method has been successfully used for modeling the mechanical behaviour of metallic composite materials³⁰. According to this method, the apparent stress and strain of PC-TiO₂ nanocomposite is written as follows:

$$\sigma_c = \sigma_f + \sigma_p(1 - \phi) \dots (8a)$$

$$\epsilon_c = \epsilon_f + \epsilon_p(1 - \phi) \dots (8b)$$

where, subscripts c, f and p, refers to composite, filler material and PC, respectively. Since these equations cannot be simply solved in the general condition, which comprises taking the distribution of stress and strain between the constituents into consideration, the solution is often done in some special cases¹⁷. Two extreme conditions that can be drawn here are iso-stress and iso-strain cases. The former case that is $\sigma_c = \sigma_f = \sigma_p$, is achieved when the filler bars are perpendicular to the force axis or in the case of the well distributed nanoparticles. This equation is also satisfied when two materials with very different mechanical strengths are mixed. The iso-strain case is attained when the applied stress gives rise to nearly identical strains in the matrix and the filler materials. This case is satisfied only when the constituents has comparable mechanical strengths.

In iso-strain condition, Eq. (8a) can be written as:

$$\epsilon_c E_c = \epsilon_f E_f + \epsilon_p E_p(1 - \phi) \dots (9)$$

As $\epsilon_c = \epsilon_f = \epsilon_p$, therefore, the following equation is resulted between the elastic modulus:

$$E_c = E_f + E_p(1 - \phi) \dots (10)$$

And then,

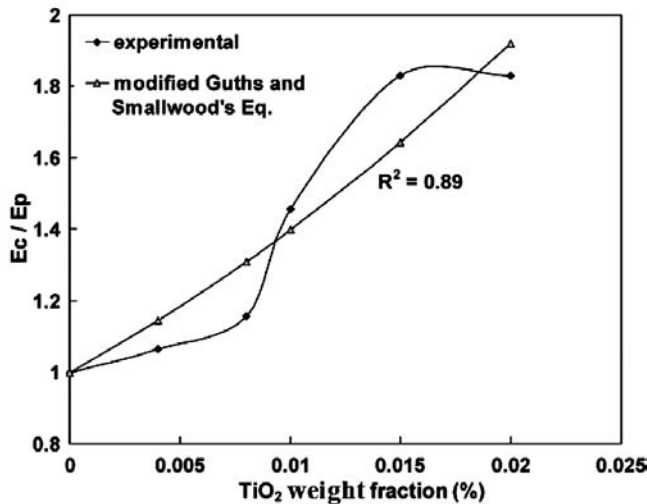


Fig. 6 – Plot of relative tensile modulus (E_c/E_p) against weight fraction of TiO_2 (Experimental data points are compared with predicted ones by modified Guth and Smallwood's equation for the studied nanocomposite)

$$\frac{E_c}{E_p} = \frac{E_f}{E_p} + (1 - \phi) \dots (11)$$

On the other hand, in iso-stress condition, from Eq. (8b) one can write:

$$\frac{\sigma_c}{E_c} = \frac{\sigma_f}{E_f} + \frac{\sigma_p}{E_p}(1 - \phi) \dots (12)$$

By applying the condition of iso-stress ($\sigma_c = \sigma_f = \sigma_p$) to Eq. (12), the Eq.(13) between modulus is obtained:

$$\frac{E_c}{E_p} = \frac{E_f}{E_p + E_f(1 - \phi)} \dots (13)$$

Figure 7 shows the results obtained from the law of mixture and indicate that for low TiO_2 contents (actually below 0.8 wt%), the experimental data are near to the iso-stress condition. In this case, sparsely distributed nanoparticles and the matrix are subjected to nearly identical stress. At higher TiO_2 contents, the behaviour of PMC is between two extreme conditions of iso-stress and iso-strain. This finding shows that at high contents of TiO_2 nanoparticles, applied stress and strain are distributed between the particles and the matrix. For a given value of TiO_2 nanoparticles, the contribution factor (CF) of iso-stress and iso-strain conditions can be determined using the following equations:

$$CF_{strs} = \frac{y_{strn} - y_{ex}}{y_{strn} - y_{strs}} \dots (14a)$$

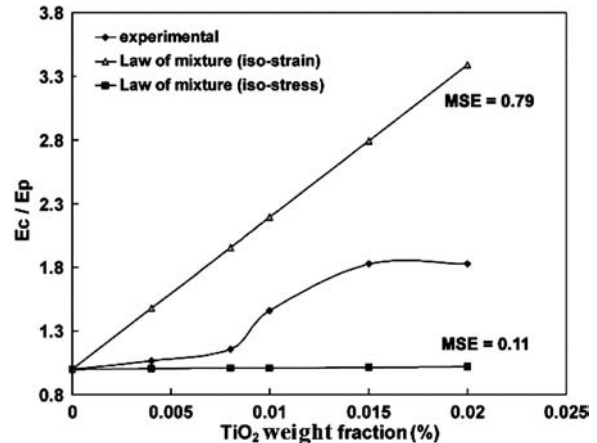


Fig. 7 – Variation of relative tensile modulus (E_c/E_p) with the weight percent of TiO_2 compared with predicted values by the law of mixture at two extreme conditions of iso-stress and iso-strain

$$CF_{strn} = \frac{y_{ex} - y_{strs}}{y_{strn} - y_{strs}} \quad \dots (14b)$$

where, y_{strn} , y_{ex} and y_{strs} , denote the values of (E_c/E_p) under iso-strain, experimental and iso-stress conditions, respectively. It is clear that the sum of these contribution factors will be equal to unity (i.e. $CF_{strn} + CF_{strs} = 1$). For example, for PC-TiO₂ (0.8 wt%), the values of y_{strn} , y_{ex} and y_{strs} are 1.96, 1.008 and 1.156, respectively; and CF_{strs} and CF_{strn} are determined as 0.82 and 0.18, respectively. When TiO₂ nanoparticles weight fraction exceeds 0.8 wt%, CF_{strn} increases (e.g. 0.46 at weight fraction of 1.5 wt%). This means that the contribution of particles in the total elastic strain of the composite increases as their value rises. However, it is observed that even for PC-TiO₂ (2 wt%), the contribution of particles in the total elastic strain is as low as 1/2 that is due to the sharp difference between the elastic modulus of TiO₂ (about 152 GPa) and PC (1.26 GPa). Hence, 0.8 wt% TiO₂ is a critical value that causes a kind of strain transfer to the particles. In fact, at lower values of TiO₂ nanoparticles, most of the elastic deformation is accommodated by the softer phase that is PC. However, when the value of TiO₂ exceeds 0.8 wt%, some of elastic strain, is accommodated by the filler particles. Figure 6 shows the calculated values of CF_{strs} and CF_{strn} as functions of TiO₂ nanoparticles weight fraction. It is interesting that for PC-TiO₂ (2 wt%), the experimental data again tends to the iso-stress condition. This can be attributed to the stress concentration that is originated from the particles and increases the stress applied on the polymeric chains of molecules between them. It can, therefore, be inferred that with increasing the weight fraction of nanoparticles, their stress concentration plays a greater role in the mechanical properties of the composite. The variations of CF_{strs} and CF_{strn} with the value of TiO₂ nanoparticles have been well fitted with third order polynomial curves as shown in Fig. 8.

The experimental value of E_c/E_p for a PMC can be predicted using the Eq. (15):

$$\frac{E_c}{E_p} = CF_{strn} \cdot \left(\frac{E_c}{E_p}\right)_{strn} + CF_{strs} \cdot \left(\frac{E_c}{E_p}\right)_{strs} \quad \dots (15)$$

where, $(E_c/E_p)_{strn}$ and $(E_c/E_p)_{strs}$ are determined from Eqs (11) and (13), respectively. Figure 9 shows a comparison between the experimental data and the values predicted by the law of mixture technique. It is evident that this technique gives a better prediction of

the experimental results. This is due to the fact that the law of mixture technique is a physical based model that uses the mechanical properties of the constituents as the entering data.

3.2 Tensile stress and strain analyses

The tensile stress and strain of the PMC have been determined at the peak of the obtained stress-strain curves. The peak is important because it is the onset of material weakening that finally leads to fracture. It is, generally, accepted that adding a filler material

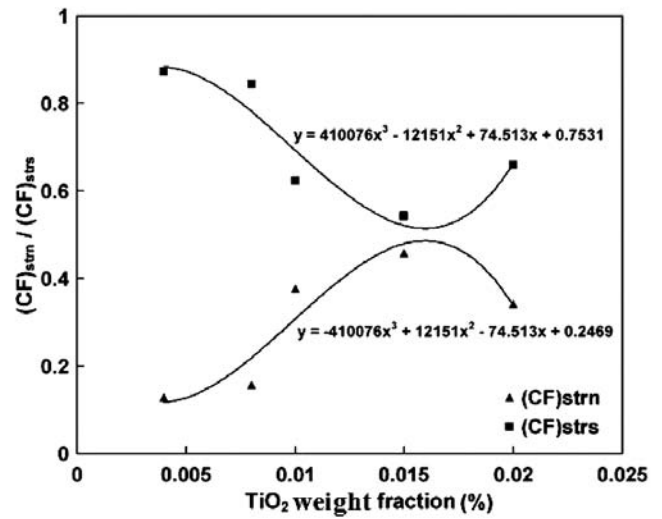


Fig. 8 – Contribution factors of iso-stress (CF_{strs}) and iso-strain (CF_{strn}) conditions calculated using Eqs. (14a) and (14b) as functions of the value of TiO₂ (Calculated data have been well fitted with third order polynomial curves)

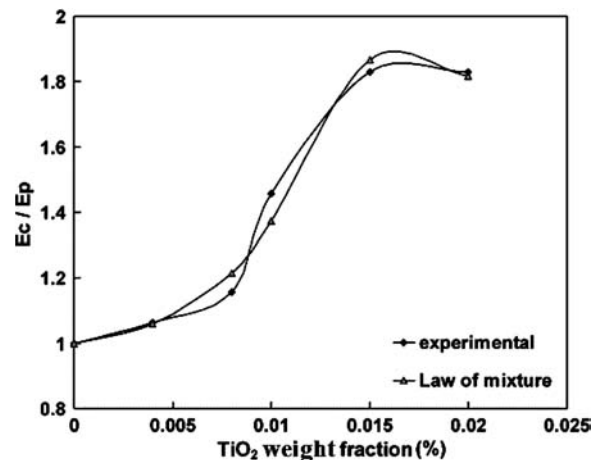


Fig. 9 – Plot of relative tensile modulus (E_c/E_p) against the weight fraction of TiO₂ (Experimental data points are compared with the predictions made by the law of mixture modeling)

with greater stiffness to a soft matrix will increase the yield strength of the composite. However, the same conclusion is not always obtained about the peak strain. Figure 10 shows the experimental peak stress and strain for the studied PMC versus the weight fraction of TiO_2 . It is manifest that the addition of 2 wt% TiO_2 to PC could increase the strength level as high as 18%. This considerable increase in tensile strength is associated with the influence of hard TiO_2 nanoparticles on inhibiting the free flow of molecular chains of the PC matrix. Especially, at low TiO_2 nanoparticles content, the nanoparticles have very low cooperation in the elastic deformation of the composite, which in turn increase their strengthening potential. The same results have been obtained from the variation of peak strain with the weight fraction of TiO_2 nanoparticles. This interesting result implies that the elastic response of the composite material is more or less improved as compared to the pure PC, at least over the studied range of TiO_2 nanoparticles weight fractions. It is also observed that the increase of E in the studied PMC is not incorporated with brittleness. Higher peak strains in the composite material may be due to the influence of filler particles on improving the alignment of molecule chains with respect to the deformation axis. The anisotropy of the matrix at the presence of nanoparticles may help the polymeric molecules to better deform under stress. However, previous investigations^{14,16} done on composites with higher filler contents (up to 40 wt%) have reported decreasing trend of peak strain with increasing filler content. This apparent disagreement can be accounted for by considering the fact that at higher values of

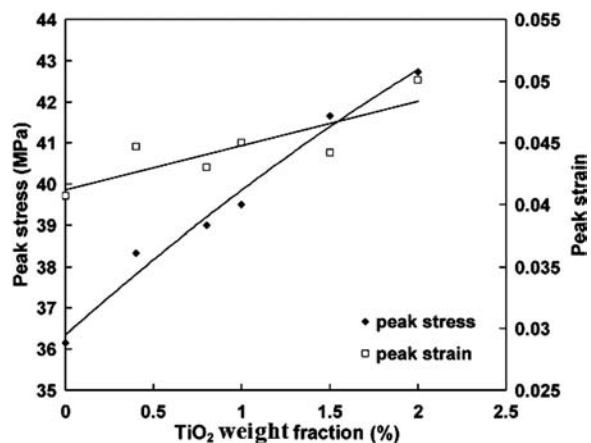


Fig. 10 – Plot of the experimental peak stress and strain for the studied PMC versus the weight fraction of filler material

filler material, filler particles weaken the structure of PMC and therefore, leads to brittleness.

Some of the most commonly used theoretical models to describe the dependence of peak or tensile stress on the weight fraction of the filler material are power law equations with different exponents¹⁵ as in Eqs. (16a)-(16c):

$$\frac{\sigma_c}{\sigma_p} = 1 - \dots (16a)$$

$$\frac{\sigma_c}{\sigma_p} = 1 - 2/3 \dots (16b)$$

$$\frac{\sigma_c}{\sigma_p} = A - B \dots (16c)$$

where, subscripts c and p, refer to the composite material and matrix, respectively. Although Eq. (16) takes the weakness of composite due to the existence of particles into account, neglect the stress concentration that exists in the narrow parts of the matrix between the particles. Nielsen^{16,31} considered the compensation for stress concentration by introducing a coefficient (S) as in Eqs (17) and (18) or by introducing a new exponential model as Eq. (19):

$$\frac{\sigma_c}{\sigma_p} = (1 -)S \dots (17)$$

$$\frac{\sigma_c}{\sigma_p} = (1 - 2/3)S \dots (18)$$

$$\frac{\sigma_c}{\sigma_p} = \exp(-a) \dots (19)$$

where, the value of a directly depends on stress concentration. Equations (17-19) all account for the weakness of the composite structure due to the existence of stress concentration at the filler-matrix interface. The models have been checked for composites with high filler contents (up to 60 wt%) and it has been proved that stress concentration due to the high weight fraction of particles plays an important role in the weakening of composite structures^{14,15}. However, the results presented in current research as shown in Fig. 10 provide evidence of the strengthening influence of the filler material when the weight fraction of the strengthening particles is low. These observations are found to be in

agreement with the law of mixture analysis of elastic modulus presented above. The poor adhesion that is thought to exist between the filler particles and the matrix at low weight fractions decreases and the condition of iso-stress is replaced with a complex situation between iso-stress and iso-strain. The degradation of iso-stress condition gradually imposes stress concentration on the interface of the constituents and weakens the structure at higher filler contents. Figure 11 compares the experimental data with the predicted values by the modified linear and exponential models. It is clear that both models

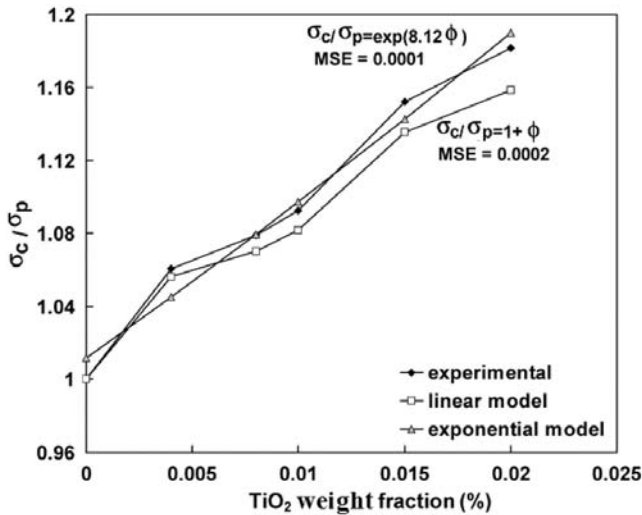


Fig. 11 – Variation of the relative tensile stress (σ_c / σ_p) with the weight fraction of TiO₂ (Experimental values compared with the results of the exponential and linear models)

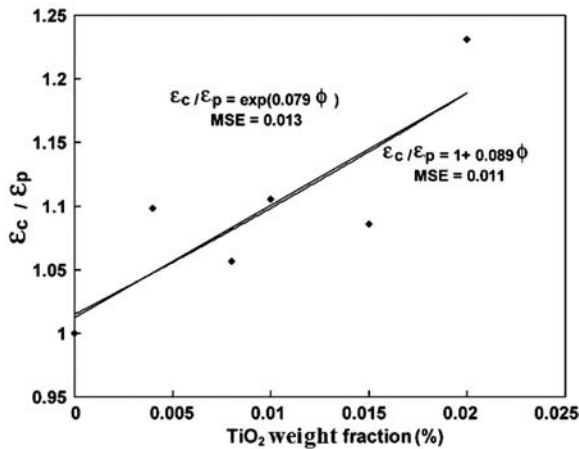


Fig. 12 – Variation of the relative peak strain (ϵ_c / ϵ_p) with the weight fraction of TiO₂ (Experimental values are compared with the results of the exponential and linear models)

provide good predictions with low MSE values and can, therefore, be used for the range of low TiO₂ nanoparticles weight fractions.

Figure 12 shows that the same model satisfactorily predict the variation of peak strain with the weight fraction of TiO₂ nanoparticles. However, higher values of MSE imply that the peak strain is more sensitive than the peak stress to some other physical parameters, such as the anisotropy of molecules and the distribution of filler particles.

Figure 13 (a and b) shows the variations of fracture stress and strain as functions of the TiO₂ value. It is worthy to note that $\sigma_{fc} / \sigma_{fp}$ (subscripts fc and fp refers to fracture in composite and pure PC matrix, respectively) tends to decrease with increasing the value of TiO₂ nanoparticles. This can be significant that when plastic deformation starts, the contribution of hard TiO₂ nanoparticles decreases and the imposed plastic strain is mostly accommodated by the softer phase that is polycarbonate. In such a case, the undeformable particles are the major source of voids

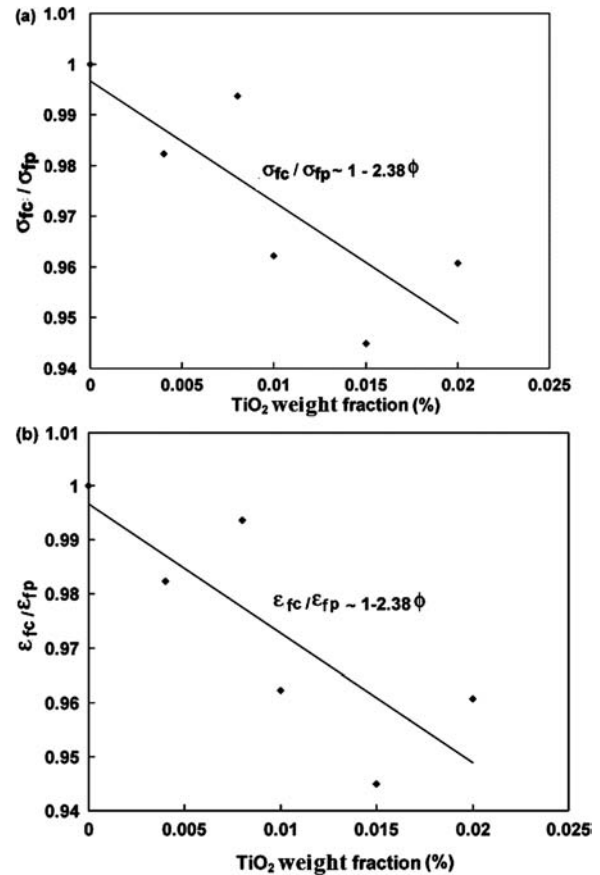


Fig. 13 – Plot of the variations of fracture stress and strain as a functions of the TiO₂ value

and cavitation in the matrix. When the weight fraction of TiO₂ nanoparticles increases, the formation of voids at the interface of particles and matrix becomes easier and needs lower fracture stress. It is also reasonable to consider more probability for cavitation and fracture when the fraction of filler increases. This signifies the decrease of fracture strain with increasing TiO₂ nanoparticles weight fraction.

4 Conclusions

The mechanical properties of PC-TiO₂ nanocomposite films have been investigated by conducting tensile tests and hardness measurements. The major results can be drawn as:

(i) The elastic modulus of PC-TiO₂ nanocomposites increases with increasing TiO₂ nanoparticles weight fraction, especially over 0.8 wt%. The results of tensile testing have been found to be in agreement with those of micro-hardness measurements.

(ii) The XRD diffraction results showed that the considerable increase of elastic module and the tensile strength of the composite can be attributed to the strengthening influence of nanoparticles as well as the crystallization of PC matrix.

(iii) The theoretical models proposed by Einstein (for complete adhesion as well as that for poor adhesion), Guths-Smallwood, Kerner and Cohen-Ishai were used but the correlation of predicted values with the experimental results have not found to be satisfactory. The best correlation was obtained from Guths-Smallwood's model and the equation was modified for the studied composite.

(iv) The law of mixture was used in the extreme conditions of iso-stress and iso-strain conditions to calculate the contribution coefficients of the constituents. The predicted values from this model have been found to be very good fitted with the experimental data points.

(v) Peak stress and strain increased with increasing TiO₂ nanoparticles content. The experimental data have been modeled by linear and exponential equations.

(vi) Unlike the peak stress and strain, the stress and strain corresponding to the fracture point have decreased with increasing the weight fraction of TiO₂ nanoparticles. It is attributed to the influence of particles on the plastic weakening of the composite.

References

- 1 Tripathi S K, Gupta A, Jain A & Kumari M, *Indian J Pure Appl Phys*, 51 (2013) 358.
- 2 Ray D K, Himanshu A K & Sinha, T P, *Indian J Pure Appl Phys*, 45 (2007) 692.
- 3 Jaleh B, Shayegani Madad M, Habibi S, Wanichapichart P & Farshchi Tabrizi M, *Surf Coat Technol*, 206 (2011) 974.
- 4 Tan E P S & Lim C T, *Compos Sci Technol*, 66 (2006) 1102.
- 5 Sharma S, Bajpai R & Chandra B P, *Indian J Pure Appl Phys*, 43 (2005) 34.
- 6 Jaleh B & Shahbazi N, *Appl Surf Sci*, 313 (2014) 251.
- 7 Subedi D P, Madhup D K, Adhikar K & Joshi U M, *Indian J Pure Appl Phys*, 46 (2008) 540.
- 8 Kumar R & Prasad R, *Indian J Pure Appl Phys*, 44 (2006) 9.
- 9 Arrier U O A & Tepehan F Z, *Surf Coat Technol*, 206 (2011) 37.
- 10 Sankar S & Gopchandran K G, *Indian J Pure Appl Phys*, 46 (2008) 791.
- 11 El-Batal & Fatma H, *Indian J Pure Appl Phys*, 47 (2009) 631.
- 12 Badr Y, Battisha I K, Salah A & Salem M A, *Indian J Pure Appl Phys*, 46 (2008) 706.
- 13 Hsieh A J, Moy P, Beyer F L, Madison P, Napadensky E, Ren J & Krishnamoorti R, *Polym Eng Sci*, 44 (2004) 825.
- 14 Tavman H, *J Appl Polym Sci*, 62 (1996) 2161.
- 15 Maltl S N & Lopez B H, *J Appl Polym Sci*, 44 (1992) 353.
- 16 Maw S N & Mahapatro P K, *J Appl Polym Sci*, 42 (1991) 3103.
- 17 Chow T S, *J Mater Sci*, 15 (1980) 1873.
- 18 Badapanda T, Senthil V, Anwar S, Cavalcante L S, Batista N C & Longo E, *Appl Phys*, 13 (2013) 1490.
- 19 Sökmen M, Tatlıdil I, Breen C, Clegg F, Buruk C K, Sivlim T & Akkan S, *J Hazard Mater*, 187 (2011) 199.
- 20 Song Y S & Youn J R, *Polymer*, 47 (2006) 1741.
- 21 Han Y & Elliott J, *Comput Mater Sci*, 39 (2007) 315.
- 22 Gueguen O, Ahzi S, Makradi A & Belouettar S, *Mech Mater* 42 (2010) 1.
- 23 Nagy P & Vas L M, *Exp Polym Lett*, 1 (2007) 84.
- 24 Cespi M, Bonacucina G, Misici-Falzi M, Golzi R, Boltri L & Palmieri G, *Eur J Pharm Biopharm*, 67 (2007) 476.
- 25 Al-Haik M, Vaghar M R, Garmestani H & Shahawy M, *Compos Part B*, 32 (2001) 165.
- 26 Gandhe A R & Fernandes J B, *J Mol Catal A*, 226 (2005) 171.
- 27 Alberola N, Fugier M, Petit D & Fillon B, *J Mater Sci*, 30 (1995) 860.
- 28 Nie J, Jia Y, Qu P & Shi Q, *J Inorg Organomet Polym*, 21 (2001) 973.
- 29 Houshyar S, Shanks R A & Hodzic A, *Exp Polym Lett*, 1 (2009) 2.
- 30 Momeni A, Dehghani K & Poletti M C, *Mater Chem Phys*, 139 (2013) 747.
- 31 Nielsen L E, *J Comp Mater*, 1 (1967) 100.